Journal of Applied Geophysics 100 (2014) 14–22

Contents lists available at ScienceDirect

Journal of Applied Geophysics

journal homepage: www.elsevier.com/locate/jappgeo

Frequency domain electromagnetic induction survey in the intertidal zone: Limitations of low-induction-number and depth of exploration

Samuël Delefortrie [a,*], Timothy Saey [a], Ellen Van De Vijver [a], Philippe De Smedt [a], Tine Missiaen [b], Ine Demerre [c], Marc Van Meirvenne [a]

[a] Research Group Soil Spatial Inventory Techniques, Department of Soil Management, Ghent University, Coupure Links 653, B-9000 Ghent, Belgium
[b] Renard Centre of Marine Geology, Department of Geology and Soil Science, Ghent University, Krijgslaan 281, B-9000 Ghent, Belgium
[c] Flanders Heritage Agency, Koning Albert II-laan 19, B-1210 Brussels, Belgium

ARTICLE INFO

Article history:
Received 8 July 2013
Accepted 21 October 2013
Available online 30 October 2013

Keywords:
Near-surface geophysics
Electromagnetic induction
Apparent electrical conductivity
Low-induction-number
Intertidal zone
Depth of exploration

ABSTRACT

Subsurface investigation in the Belgian intertidal zone is severely complicated due to high heterogeneity and tides. Near-surface geophysical techniques can offer assistance since they allow fast surveying and collection of high spatial density data and frequency domain electromagnetic induction (EMI) was chosen for archaeological prospection on the Belgian shore. However, in the intertidal zone the effects of extreme salinity compromise validity of low-induction-number (LIN) approximated EMI data. In this paper, the effects of incursion of seawater on multi-receiver EMI data are investigated by means of survey results, field observations, cone penetration tests and in-situ electrical conductivity measurements. The consequences of LIN approximation breakdown were researched. Reduced depth of investigation of the quadrature-phase (Qu) response and a complex interpretation of the in-phase response were confirmed. Nonetheless, a high signal-to-noise ratio of the Qu response and viable data with regard to shallow subsurface investigation were also evidenced, allowing subsurface investigation in the intertidal zone.

1. Introduction

The coastal plain of Belgium is situated along the southern part of the North Sea and consists of polders, dunes and a shore. The western part of the Belgian coastal plain bears a thick Holocene sequence which is made up of alternating clastic and biogenic layers that are not consolidated (Baeteman, 1991). Besides the influence of natural processes on the subsurface, human intervention has been established as an important factor. Regarding human intervention in the coastal plain the industrial activities in pre-Roman and Roman times are of special interest due to intensive peat extraction and saltmaking (van den Broeke, 1996).

Conventionally, archaeological site investigation in the intertidal zone in Belgium has relied solely on information derived from boreholes, trenches, surface findings and (aerial) photographs. In the past visual observation of archaeological traces and surface findings have been most successful following storm surges which were powerful enough to remove sediment overlying deposits of archaeological interest. At present this is often no longer possible because many groynes were constructed in the seventies of the last century to halt excessive sediment erosion of beach sands by longshore currents. Thus archaeological traces often remain buried.

Invasive exploration in the intertidal zone is complicated due to a high groundwater table, strong groundwater flow, presence of loose sand, semi-diurnal tides and multiple tidal constituents. Because archaeological zones of interest are only approximately delineated and semi-diurnal tides occur, the ability to gather high resolution spatial data in a rapid manner is desirable. Additionally the occurrence of unexploded ordnances of both world wars poses a potential hazard and investigation would be preferably non-invasive. Several geophysical techniques are then eligible, yet the saline character of the intertidal zone is again a restricting factor. For example, ground penetrating radar does not work well in saline/brackish coastal environments because of signal dissipation and loss (Buyvenich et al., 2009). The viability of electromagnetic induction (EMI) data is also doubtful when using low-induction-number (LIN) approximation because of a limited dynamic range (Callegary et al., 2007; McNeill, 1980). Yet EMI has been successfully employed for the delineation of traces of archaeological interest (Simpson et al., 2009a) and assessment of palaeo-landscapes (De Smedt et al., 2011) in various geological settings. Moreover, EMI sensors have been used as a soil salinity sensor (e.g. de Jong et al., 1979; Hendrickx et al., 1992; Williams and Baker, 1982).

In this paper, the effects of incursion of seawater are discussed together with the viability of EMI as a prospection technique in the intertidal zone. The influence of extreme salinity on the responses of the sensor is investigated. Concerns such as biased data because of LIN approximation and uncertainty of the depth of investigation are researched as well. Results are validated with information from

* Corresponding author. Tel.: +32 9 264 58 69; fax: +32 9 264 62 47.
E-mail address: Samuel.Delefortrie@UGent.be (S. Delefortrie).

0926-9851/$ – see front matter © 2013 Elsevier B.V. All rights reserved.
http://dx.doi.org/10.1016/j.jappgeo.2013.10.005

augerings, cone penetration tests (CPT) and in-situ electrical conductivity measurements.

2. Study area

The study area is located in the intertidal zone, near Raversijde, Belgium (Fig. 1) and is about 8 ha in size. The survey zone was demarcated by the sea during neap tide to the Northwest, by the levee to the Southeast and by groynes laterally. The beach has a low-angle dip with a mean slope of about 1.7%. Fig. 1B shows the elevation (mTAW, where TAW stands for "Tweede Algemene Waterpassing") of the study area. 0 mTAW is the Belgian reference datum level referring to the mean low low sea-water level.

The subsurface consists of Quaternary deposits comprised of clastic (beach sands and fine-grained mudflat sediments) and biogenic (peat) deposits which overlie Pleistocene deposits. The site was chosen for archaeological prospection mainly because of evidence of past peat extraction; an oblique aerial photograph taken after a storm event and before the construction of the groynes revealed traces thereof. Orthorectification and georeferencing of this photograph was performed (Fig. 1C). Controlled detonation of shells after burying has taken place near the low water line in the study area from the late 90s until recently. Unfortunately, information about quantity and exact locations is not available.

3. Materials and methods

3.1. EMI

EMI instruments produce a time-varying electromagnetic (EM) field, thereby inducing EM fields in the subsurface and measure the resulting field, which has a quadrature-phase (Qu) component and in-phase (Ph) component, expressed in parts per thousand.

The Qu response is converted to ECa, expressed as mS m^{-1}, using the formula (McNeill, 1980):

$$ECa = \frac{2}{\pi f s^2 \mu_0} \cdot \left(\frac{\mathbf{H}_s}{\mathbf{H}_p}\right)_{Qu}$$

where f is the frequency (Hz), s is the coil separation (m), μ_0 is the magnetic permeability of free space ($4\pi 10^{-7}$ H/m) and $(\mathbf{H}_s / \mathbf{H}_p)_{Qu}$ is the Qu component of the secondary $\mathbf{H}_s$ to primary $\mathbf{H}_p$ magnetic field coupling ratio. The formula is an approximation based on the assumption of operating the instrument in a LIN environment with zero instrument elevation. ECa as used throughout this article therefore denotes LIN approximated ECa. The dimensionless induction number is defined as the ratio of the instrument coil separation divided by the skin depth δ. The skin-depth in turn is defined as the distance within a half-space wherein a plane wave is attenuated by 1/e (37%) of the value at the surface (Spies, 1989). As the true conductivity increases, the skin depth decreases causing the induction number to rise. This effect is enhanced with increasing intercoil spacing. At high values of true conductivity the Qu response is then no longer linearly proportional to true conductivity. ECa becomes biased as the true conductivity is increasingly underestimated for a given frequency and intercoil spacing (McNeill, 1980). It has been demonstrated that, as a consequence, there is a potential risk for spatially distorted data in high conductivity environments (Beamish, 2011). However, it is unclear what the upper boundary of the induction number for a valid LIN approximation should be (Callegary et al., 2007; McNeill, 1980). Beamish (2011) notes that such discussions are not generally useful unless the coil configuration,

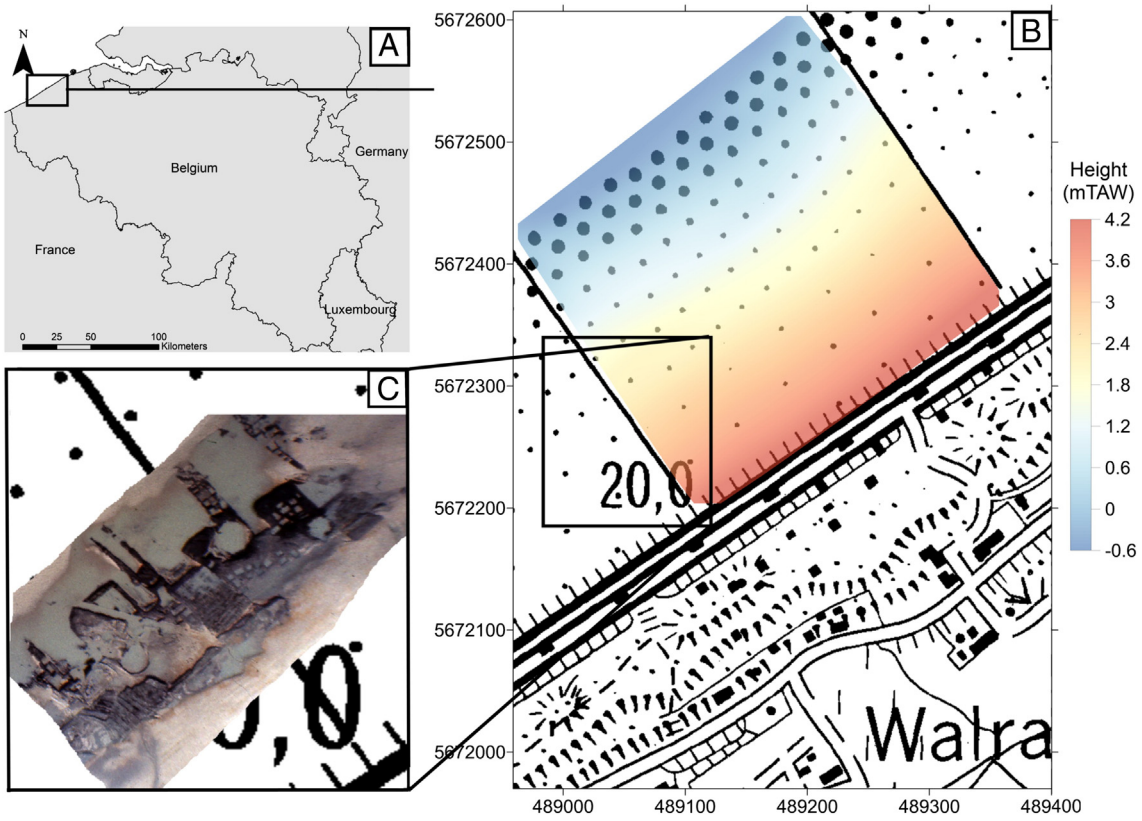

Fig. 1. (A) Location of the study area in Belgium. (B) Localization on the topographical map with elevation of the study area, coordinates are in the UTM geographic coordinate system (m). (C) Orthorectified aerial picture taken after a storm event at low tide with a view of different peat excavation features present in the subsurface (author: Etienne Cools, early 1970s, unpublished). The clipped toponym 'Walra' is 'Walraversijde' in full.

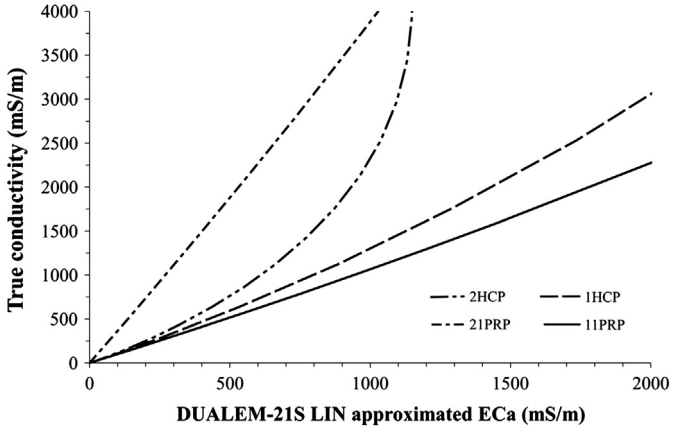

Fig. 2. Relation between the LIN approximated ECa and ECa* for the DUALEM 21S coil configurations.

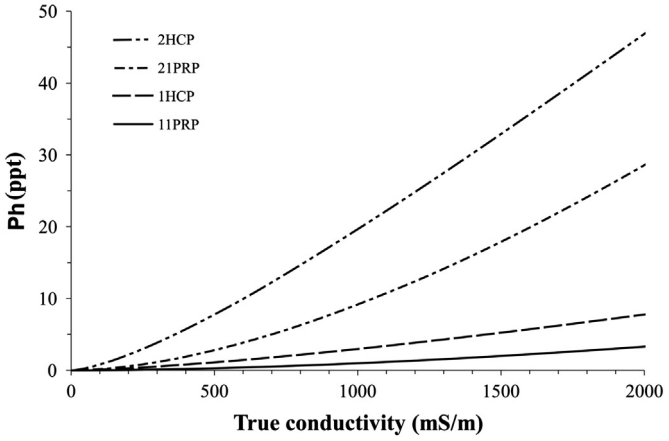

Fig. 3. Relation between the Ph response and ECa* for the DUALEM 21S coil configurations.

the instrument elevation and the required accuracy (of true conductivity) are all considered.

Assuming zero elevation (of the inter-coil centre line above ground surface) and free-space magnetic susceptibility, tabulations of the Qu and Ph responses with increasing induction number have been published by Frischknecht (1967) for the HCP and PRP coil geometries, using Wait's (1982) developments on the response of dipole–dipole systems at the surface of the earth. These tabulations can be used to calculate the theoretical deviation of the linear relation between ECa and true conductivity with increasing conductivity. Fig. 2 shows the theoretical deviations for the coil configurations of the sensor used; the DUALEM 21S (DUALEM Inc., Milton, Canada).

Beamish (2011) proposed a correction procedure involving a least-squares polynomial fitting to the theoretical deviation of the linear relationship between LIN approximated ECa and true conductivity for the coil configurations to allow for correction of the LIN approximation breakdown. This approach has been adopted in this article and the corrected LIN approximated ECa will be referred to as the estimated true apparent electrical conductivity (ECa*) because of the theoretical background of the correction procedure. The ECa ranges of the data measurements were taken into account to ensure a good fit over the data intervals. The coefficients for the polynomials ($a_0 + a_1x^1 + a_2x^2 + a_3x^3$) used are listed in Table 1.

The Ph response is the sum of a response proportional to the magnetic susceptibility and of a response due to conductivity which becomes important only in the case of low resistivity values (Tabbagh, 1986). Thus the Ph response can no longer be linked to the magnetic susceptibility of the subsurface when high conductive deposits prevail. Since Frischknecht (1967) also tabulated the Ph response with increasing induction number for the HCP and PRP coil geometries, the theoretical response solely due to increase in true conductivity can be presented as well (Fig. 3).

Multi-receiver, frequency domain EMI data were collected using a DUALEM 21S sensor in a mobile set-up. The sensor has an operating frequency of 9 kHz and has four coil configurations; i.e. one transmitting coil paired with four receiving coils of which two perpendicular (PRP) coil configurations (11PRP and 21PRP) with 1.1 and 2.1 m intercoil spacings and two horizontal coplanar (HCP) coil configurations (1HCP and 2HCP) with an intercoil spacing of 1 and 2 m respectively. This allows for the near simultaneous recording of four different subsurface volumes. The depth of exploration (DOE) is defined as the depth at which 70% of the total signal response is obtained from the soil volume above this depth and differs according to coil configuration and intercoil spacing. The DOE of the Qu response for the 11PRP, 21PRP, 1HCP and 2HCP are respectively around 0.5, 1, 1.5 and 3.2 m below the sensor inter-coil centre line when LIN conditions are valid. Note that as the skin depth decreases in high conductive environments so does the DOE (Callegary et al., 2007). The instrument elevation (inter-coil centre line) was 0.16 m and the sampling frequency was 8 Hz. The data were collected along parallel lines, 2 m apart, with an in-line resolution of approximately 0.25 m. A smaller spacing between lines is recommended for archaeological prospection of small-scale features but the 2 m spacing was a trade off between spatial resolution necessary for archaeological surveys and collection speed necessary for measuring in the intertidal zone. A 2 m spacing between lines does imply a focus on larger phenomena. Geographic coordinates were logged using a dGPS system. The soil temperature measured during the survey was 7.2 °C. ECa measurements depend on the soil temperature and for reasons of comparison they may be standardized according to a reference temperature. Usually a reference temperature of 25 °C is taken (Slavich and Petterson, 1990):

$$ECa(25^{\circ}C) = ECa \cdot \left(0.447 + 1.4034 \cdot e^{-T/26.815}\right)$$

with ECa (25 °C) the standardized ECa at a temperature of 25 °C and T the soil temperature in °C.

After collection, the ECa and Ph data were corrected for instrument drift and interpolated using ordinary kriging (Goovaerts, 1997). A detailed overview of the drift correction procedure can be found in Simpson et al. (2009b).

Drift correction was applied to all data presented in this paper. Unless mentioned otherwise, no other corrections such as accounting

Table 1
Coefficients of the least-squares polynomials fitted to the theoretical deviation of the linear relationship between LIN approximated ECa and true conductivity. The determination coefficients (R^2) of the fitted polynomial expressions are listed in the last column.

	a_0	a_1	a_2	a_3	R^2
11PRP	2.50505E−02	9.96478E−01	6.76400E−05		1
21PRP	2.50254E+00	9.83832E−01	3.14400E−05		0.999992
1HCP	−2.58679E+00	1.07515E+00	2.22768E−04		0.999998
2HCP	2.208980E+01	1.329896E+00	1.033999E−05	8.971238E−07	0.999988

for temperature, instrument elevation or LIN approximation breakdown were performed.

In a two-layered subsurface model, the relationship between the lower boundary of the upper layer (z) and the ECa can be modelled by formulating the cumulative response $R_h(z)$ for the HCP coil orientation. Depths are normalized by dividing the z by the intercoil spacing s to remove the effect of differences in intercoil spacing into the cumulative response function $R_h(z)$ (Morris, 2009):

$$R_h(z) = \alpha_h \cdot e^{-\beta_h \cdot \left(\frac{z}{s}\right)}$$

with α_h and β_h the unknown parameters of the exponential cumulative response function for the HCP coil configuration $R_h(z)$. These unknown parameters α_h and β_h can be empirically determined by fitting the cumulative response function $R_h(z)$ to the z & 1HCP ECa and z & 2HCP ECa observations. The detailed overview of the procedure is described by Saey et al. (2011).

3.2. Validation

Hand augerings were performed to validate the EMI-measurements. A combination of Edelman augers, a bailer sampler and casing were used. In addition, 100 kN electrical CPT's were carried out. The used CPT probe had a cross-sectional area of 10 cm^2 and measured the cone resistance (total force acting on the cone divided by the projected area of the cone), qc, and the sleeve friction (total force acting on the sleeve of the cone divided by the area of the sleeve), fs, simultaneously. Soil properties such as composition, grain size, and soil consolidation govern qc and fs (Lunne et al., 1997). A qc measurement at a particular depth is influenced by a volume of a few cone diameters around the tip (Robertson and Campanella, 1983).

An EC-probe for soil conductivity measurements was also used. It consists of a borehole earth resistivity metre (Eijkelkamp Agrisearch Equipment, Giesbeek, The Netherlands). Measurement of the soil resistivity using four electrodes is based on the Wenner method, applied by Rhoades and Van Schilfgaarde (1976). It allows the measurement of the electrical resistivity in situ (which is the inverse of EC) of a soil volume of 80 cm^3 of soil around the probe. A temperature sensor is also present to convert the measurements to the reference temperature of 25 °C.

4. Results and discussion

4.1. ECa and ECa*

The ECa data (Fig. 4) evidence a high lateral and vertical variability and there are many notable anomalies. The zones near the groynes and the levee (Fig. 4) show strongly elevated or lowered ECa values which have low spatial autocorrelation. These zones are likely disturbed by the presence of building materials from the adjacent structures and were not withheld for validation, descriptive statistics or further data examination. Most notably is the central, high conductivity zone that is contrasted by lower conductivity deposits at its northwestern limit and contains small-scale linear, lower conductivity features. A trend of increasing conductivity seawards can also be discerned, present on a

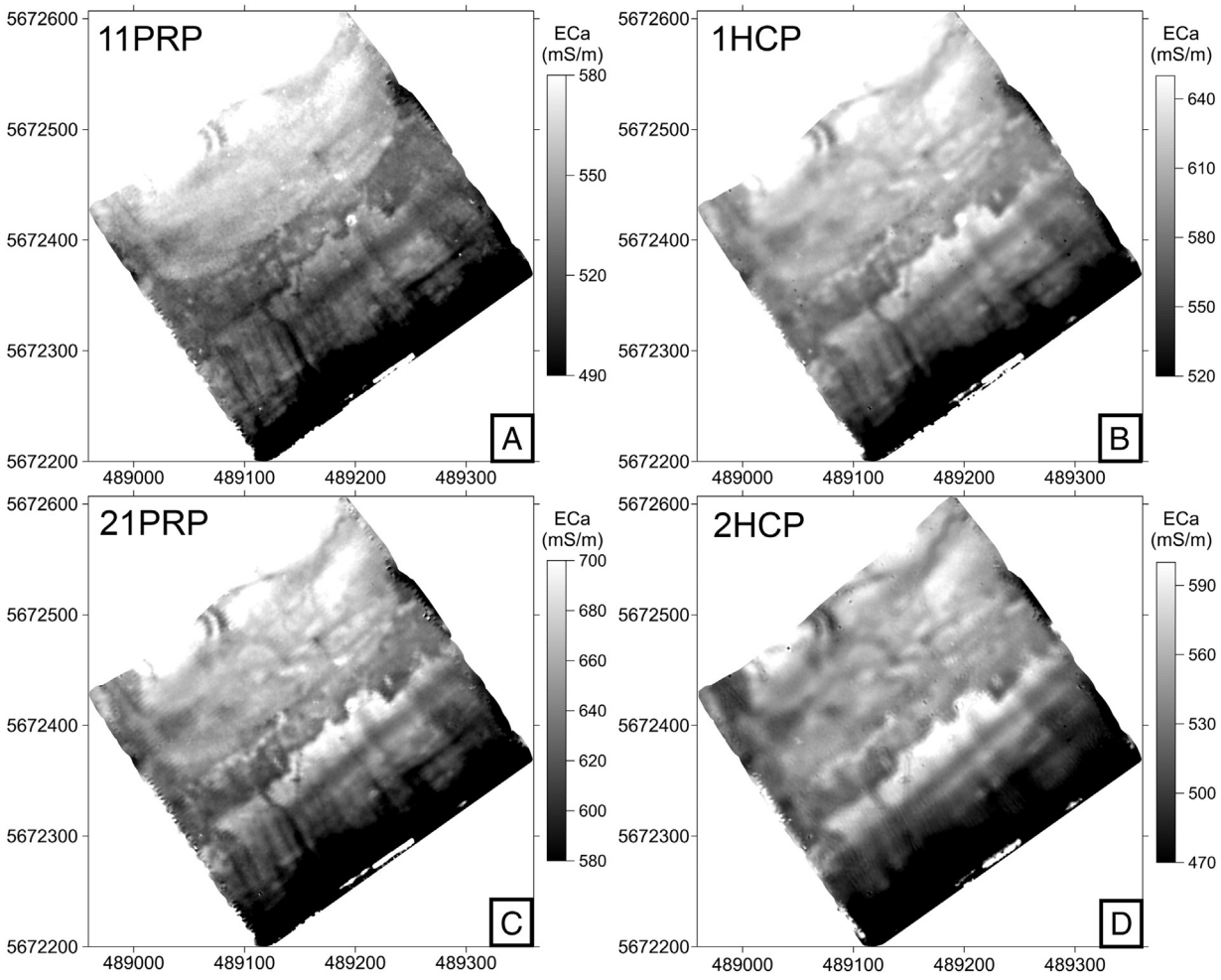

Fig. 4. Interpolated and drift corrected ECa for the DUALEM 21S coil configurations: (A) 11PRP, (B) 1HCP, (C) 21PRP, (D) and 2HCP. The colour scales do not show the full ranges of the data and differ for the coil configurations.

scale that comprises the entire study area. The contrast between the anomalies is less pronounced for the 11PRP data, indicating that the high variability in the area is mainly due to the variability in the deposits at a depth deeper than the depth of investigation of the 11PRP coil configuration.

Certain anomalies in the 2HCP data have tripled compared to the 1HCP data. Fig. 5 illustrates a small-scale, linear, low conductive feature in the central, high conductive zone in the 1HCP data, that can be seen as two low conductive linear features with a higher conductive zone in between in the 2HCP data. A HCP response (Qu) which is comprised of three extrema (one in the centre of the opposite sign and two on both sides with the same sign as that of the contrast) has been demonstrated by Frischknecht et al. (1991) when considering a thin plate model where the strike of the plate (with low to high dip) is normal to the traverse. Notable here is that the 1HCP and 2HCP responses differ, indicating that a lateral heterogeneity smaller than the sample volume of the HCP coil configuration may result in a three-lobed response along a traverse. The ECa may then not be representative of the arithmetic average of EC within the sample volume. This accords with the findings by Callegary et al. (2012).

The values of the ECa data (Table 2) are elevated due to the high salinity and the ranges are magnified as well, compared to measurements taken in salt-free environments (e.g. Saey et al., 2009). When comparing the descriptive statistics of the ECa and ECa* data it is clear that the correction for LIN approximation breakdown has resulted in an additional amplification of the ECa* data. Furthermore, the mean conductivity increases with increasing depth investigation of the coil configuration for the ECa* data but not for the ECa data. The ECa data misrepresents the increase in conductivity with increasing depth due to increasing LIN breakdown and this advocates the need for a correction.

As the 2HCP ECa data suffers most from the LIN approximation breakdown, this coil configuration was elected for visual comparison of the ECa and ECa* data (Fig. 6). Contrary to the findings of Beamish (2011) it is clear that no spatial distortion was introduced due to the LIN breakdown despite a necessary adjustment of the colour scale.

4.2. Signal-to-noise ratio of ECa

A recording of the drift corrected ECa data was made at a fixed location during a short interval of time (Fig. 7). The ECa means and standard deviations are: 566.1 ± 0.25 mS/m (11PRP), 676.4 ± 0.23 mS/m (21PRP), 629.8 ± 0.19 mS/m (1HCP) and 565.4 ± 0.21 mS/m (2HCP). The ranges based on this recording are between 1.1 and 1.9 mS/m. Resembling the results obtained by Beamish (2011) in a similar environment, this signifies that the noise level of the recording is comparable to measurements in a low-conductive environment. Thus the salinity results in an amplified Qu response but does not significantly affect the noise level or accuracy, resulting in a higher signal-to-noise ratio.

Table 2
Descriptive statistics (m: mean, min: minimum, max: maximum, std: standard deviation) of the ECa (mS/m), ECa* (mS/m) and ECa*(25 °C) (mS/m) for the DUALEM 21S coil configurations for the study area (respectively 132,708, 132,704, 132,782, 132,887 measurement points for the 11PRP, 21PRP, 1HCP and 2HCP coil configurations).

	11PRP			21PRP		
	ECa	ECa*	ECa* (25 °C)	ECa	ECa*	ECa* (25 °C)
max	686.1	692.3	1052.3	791.0	830.6	1262.4
min	188.3	188.8	287.0	265.8	269.7	409.9
m	532.3	535.1	813.3	639.8	665.4	1011.4
std	35.5	36.0	54.8	44.8	48.3	73.5
	1HCP			2HCP		
	ECa	ECa*	ECa* (25 °C)	ECa	ECa*	ECa* (25 °C)
max	717.2	883.1	1342.2	660.7	1119.9	1702.1
min	227.6	253.6	385.5	214.0	271.7	413.0
m	592.2	712.7	1083.3	531.4	824.8	1253.6
std	41.6	55.2	83.9	42.6	86.9	132.0

4.3. In-phase response

Visual comparison of the Ph response data (Fig. 8) and the ECa data shows a good similarity and evidences the influence of conductivity on the Ph response. Despite the similarity, many point anomalies not present in the ECa data occur in the Ph data, signifying additional information on the subsurface might be gathered. The relation between 2HCP Ph and 2HCP ECa* data is shown in Fig. 9. The match with the estimated Ph response due to conductivity is limited. At the start and near the end of the survey the relation between Ph and ECa* for all coil configurations deviates from a linear relationship.

4.4. Validation

4.4.1. Augerings

Hand augering allowed for an invasive investigation of the prevailing, shallow deposits. 17 augerings were performed. In general, the study area consists of an uppermost layer of coarse to medium-grained sands with calcareous shell fragments which overlies clay, silt and peat layers with varying thicknesses. Some clay layers contain numerous calcareous shell fragments. The peat is somewhat dry and little dark brown fluid is released when compressed. The thickness of the upper sand layer (z_{sand}) obtained from the augerings ranged from 0.5 to 2 m and peat thickness from 0 to 1 m. All augerings (provided a depth down to 3 m was reached) evidenced a peat layer or peat inclusions.

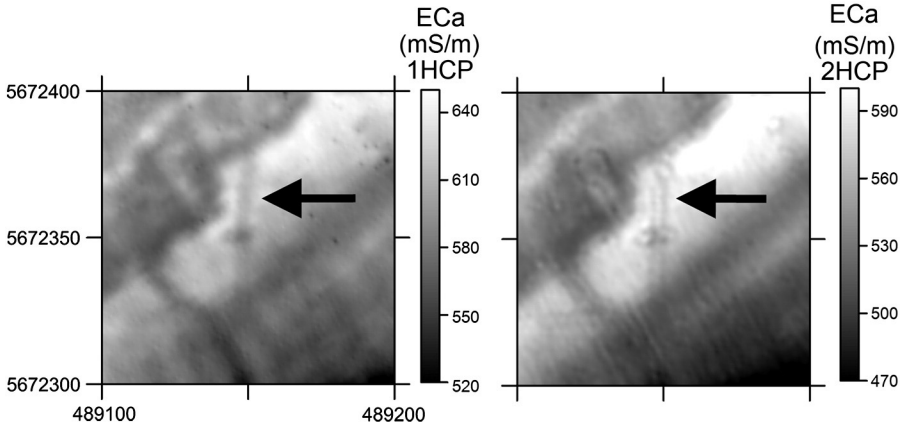

Fig. 5. Detail of tripling of a lateral heterogeneity in the study area. 1HCP (left) and 2HCP (right).

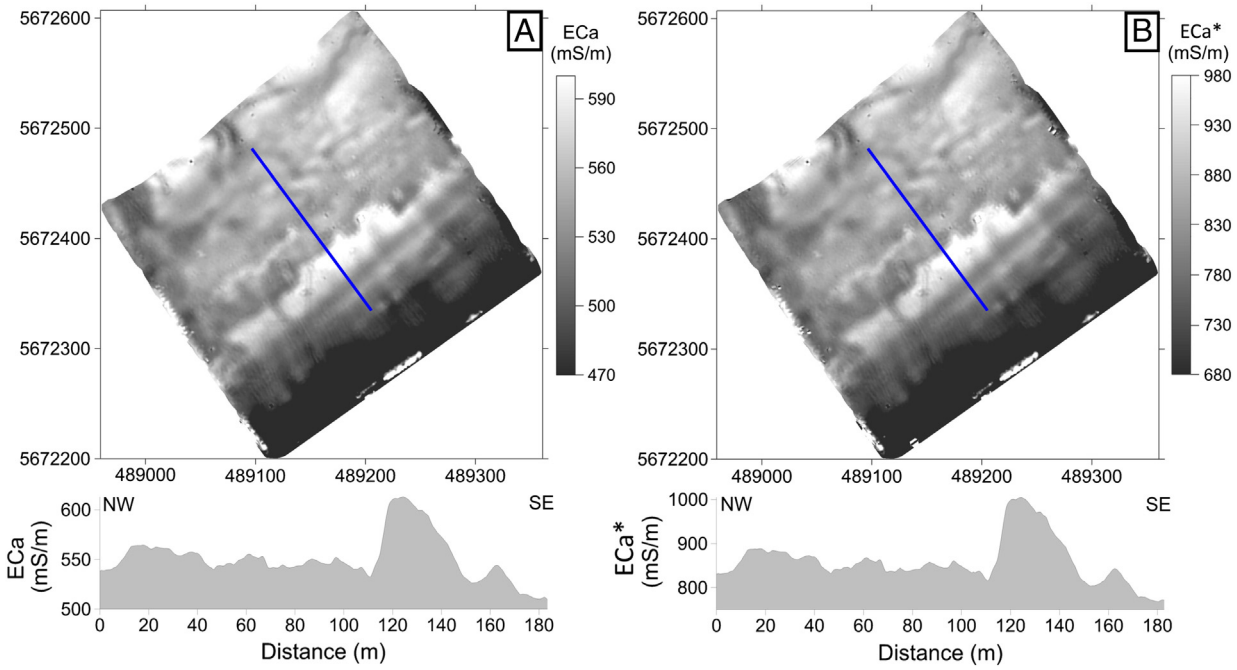

Fig. 6. (A) ECa for the 2HCP coil configuration with indication of profile 1 (below) in blue. (B) ECa* for the 2HCP coil configuration with indication of profile 1 (below) in blue. (For interpretation of the references to colour in this figure legend, the reader is referred to the web version of this article.)

The z_{sand} obtained from the augerings showed a good correlation with the 2HCP ECa* (Fig. 10) apart from outliers in zones 1 and 2 of Fig. 10. Results from 4 borings were not used due to insufficient depth penetration to reach the lower sand boundary or due to imprecise delineation of the boundary because of subtle textural differences. Significant correlation with presence or thickness of peat, clay or silt layers was not found.

Zone 1 (Fig. 10) is an area with high local ECa* variance and augerings only 2 m apart evidenced extreme heterogeneity of deposits. One augering revealed 1.4 m of clay with peat inclusions and 0.25 m of peat whereas 2 m further southeast these layers were lacking. The reason for the outlier in zone 1 is presumably caused by one or several heterogeneities smaller than the sample volume of the 2HCP coil configuration, leading to an ECa not representative of the arithmetic average of EC within the sample volume.

The correlation between the thickness of the upper sand layer and the 2HCP ECa* indicate an overall trend of increasing sand thickness landward. Yet it seems that the correlation is no longer valid near the levee (Fig. 10, zone 2). The augerings are located in the high intertidal zone. A decrease in salinity due to mixing of fresh water and sea water or a decrease in groundwater level causes a decrease in conductivity within this zone. Furthermore, it is also near the levee that a deviation from the linear relationship between the Ph response and the ECa* was noted. The data suggest a link, but sufficient evidence is not available. It does stand to reason that changes in salinity or groundwater level might affect the gradient of the relationship between Ph and ECa*. Therefore it is assumed that the linear trend found is no longer valid near the levee and near the seaward boundary of the study area.

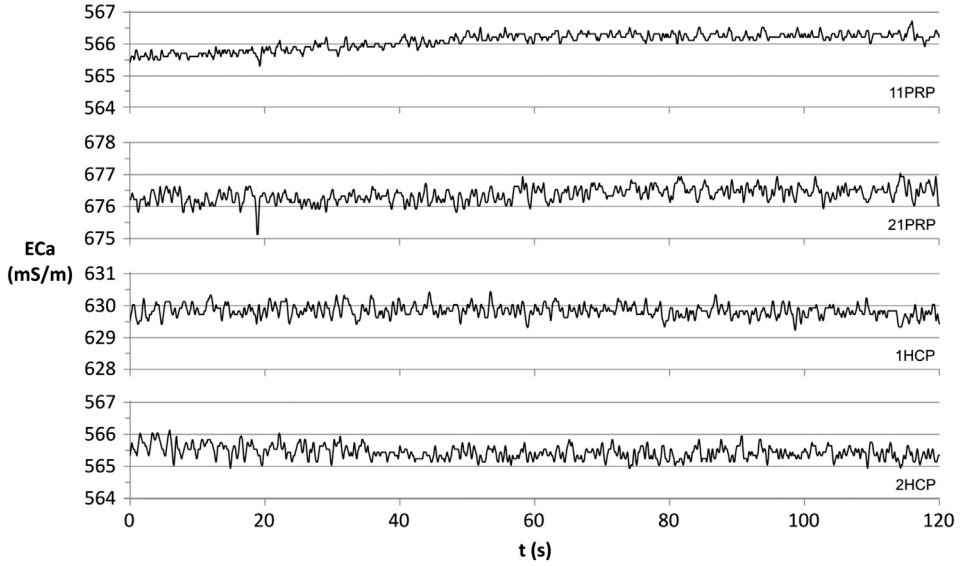

Fig. 7. Static recording of ECa for 2 min in the study area for the DUALEM 21S coil configurations (961 measurement points).

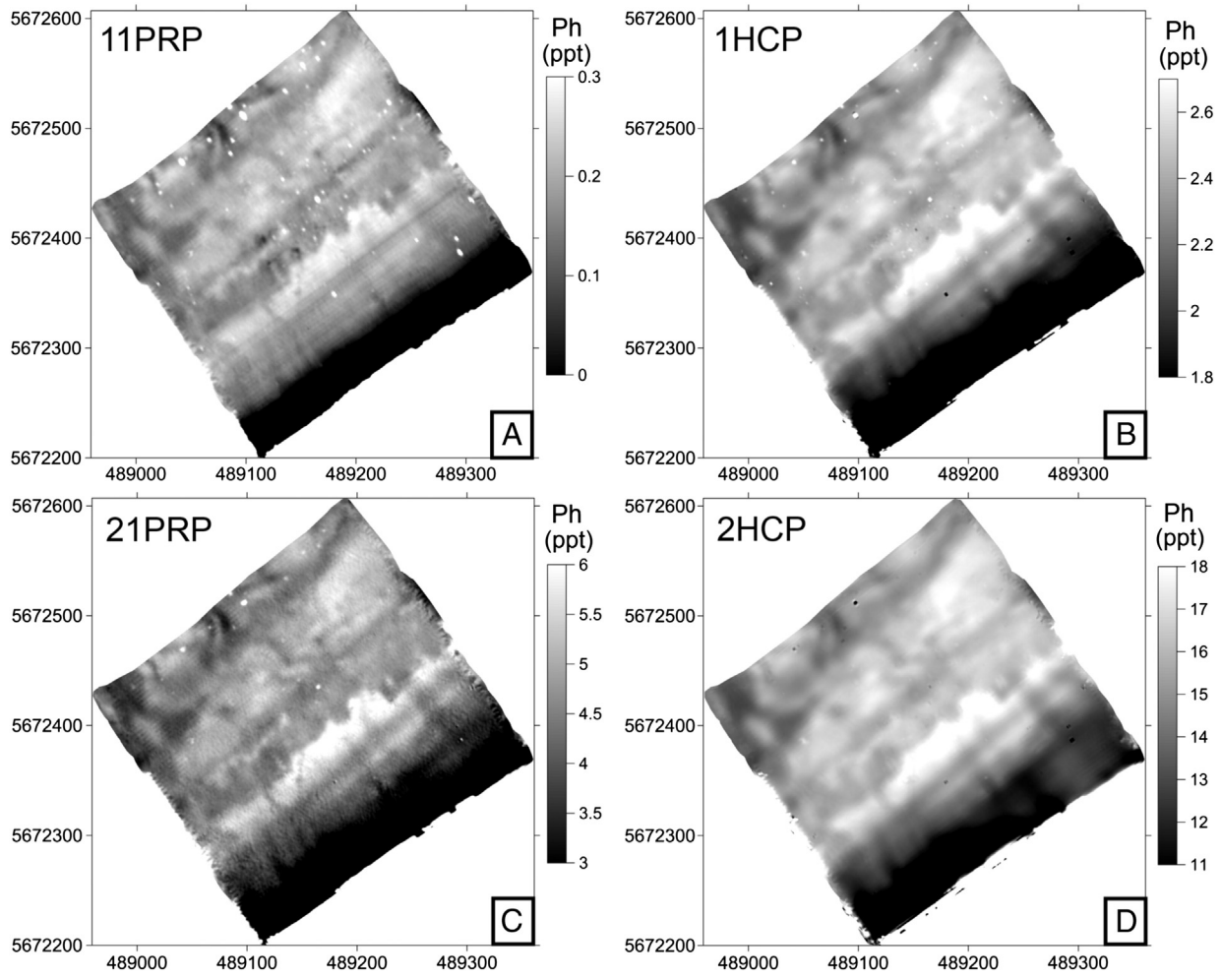

Fig. 8. Interpolated and drift corrected Ph response for the DUALEM 21S coil configurations: (A) 11PRP, (B) 1HCP, (C) 21PRP, and (D) 2HCP. The colour scales do not show the full ranges of the data and differ for the coil configurations.

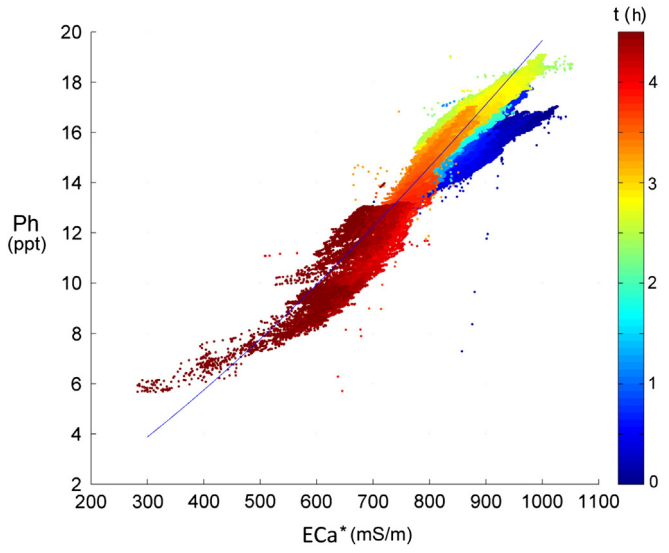

Fig. 9. Scatterplot of the Ph response and the ECa* data in the survey area. The data points are colour coded according to survey time (h). The blue curve on top is the estimated Ph response with increasing conductivity (Frischknecht, 1967).

4.4.2. CPT

The CPT parameters, *qc* and *fs* (not normalized), were used to identify the stratigraphy by using the classification proposed by Robertson et al. (1986). The first 30 cm were disregarded from classification due to the lack of compaction of the uppermost sands. The classes of the classification corresponding with gravelly sand to sand, sand, sand to silty sand and silty sand to sandy silt were interpreted as belonging to the upper beach sand cover. 14 CPT's were performed. The good correlation between z_{sand} and 2HCP ECa* was confirmed (Fig. 10). Thus validation suggests that most of the variation of the ECa* may be explained by variation in z_{sand} in the central area.

Comparison with the augerings revealed that distinguishing between clay and peat was not possible. This is likely due to inaccuracy of the *fs*. Nonetheless, comparison with the augerings did advocate sufficient accuracy of the CPT parameters for distinction of the sand layer. Presumably because the difference in *qc* of the fine-grained sediments/peat and sand is adequately large.

4.4.3. EC-probe

With the EC-probe EC (25 °C) values of the deposits present in the study area were obtained at one location (Fig. 10). The ranges for the deposits are listed in Table 3. The EC-probe measurements indicate a high contrast between clay/peat and sand. The contrast in EC between peat and clay is smaller yet peat is shown to have a higher conductivity in the study area.

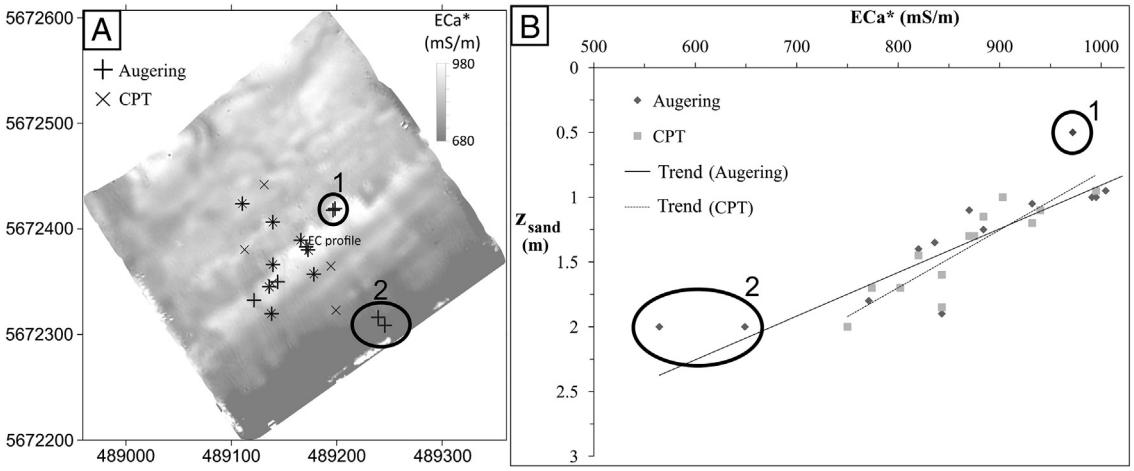

Fig. 10. (A) 2HCP ECa* map with locations of CPT's (diagonal crosses), hand augerings (crosses) and location of the EC-probe profile. (B) Scatterplot of z_{sand} and 2HCP ECa*.

In the central, large scale anomaly in the study area, characterized by high conductivity, augerings evidenced thick peat layers in. Since the conductivity of peat is the highest in the area, this anomaly is interpreted as an indication of peat. The abrupt, northwestern boundary of this area is interpreted as an extensive peat extraction boundary.

4.5. Depth of exploration

As most of the variations of the ECa* in most of the study area may be explained by variation in z_{sand}, the cumulative response curves $R_h(z)$ for the HCP coil orientations were modelled (assuming a two-layer build-up) by using the depth observation z_{sand} and the ECa*(25 °C) (Fig. 11). Since all depth observations made were between 0.9 m and 2 m, the EC of the upper layer (sand layer) and bottom layer (peat and/or fine-grained sediments) were derived from the EC-probe measurements. An ECa*(25 °C) of 950 mS/m was taken as the average value for the sand layer because the groundwater is very shallow and an ECa*(25 °C) of 1600 mS/m was taken as an average value for the clay/peat layer. The depth observations in zones 1 and 2 were not taken into account (Fig. 10).

The fitting of the depth response functions was done by minimizing the sum of the squared differences between z_{sand} and ECa* (25 °C) by iteratively altering the modelling parameters α_h and β_h for both vertical coil configurations. The optimal values of α_h and β_h were 1.1059 and 0.9771. The obtained empirical depth response curve is:

$$R_{h,s} = 1.1059 \cdot e^{-0.9771 \cdot \left(\frac{z_{sand}}{s}\right)}$$

with $R_{h,s}(z)$ the response above a depth z for the HCP coil configuration and s the transmitter–receiver coil spacing. The DOE for the fitted cumulative depth response functions were 1.18 and 2.51 m (with the sensor height considered) for the 1HCP and 2HCP coil configurations. These are respectively 0.37 m and 0.67 m more shallow as compared to DOE within the LIN range.

In numerical simulations performed by Callegary et al. (2007), the DOE decreased by up to 50% as the EC of the soil increased when compared with the predictions of the LIN approximation. Moreover, these simulations did not take into account such elevated values as encountered in the study area. When relating these results to our findings, it is clear that the reductions in DOE for the HCP coil configurations are not as pronounced (a decrease of around 25%).

Table 3
EC-probe measurements (mS/m) of the various deposits of a profile. The EC was standardized to a reference temperature of 25 °C.

Deposit	EC (25 °C)
Upper sand layer	736 (dry sand)–953 (saturated with groundwater)
Peat	1664–2025
Clay	1472–1519

5. Conclusions

EMI surveys in an extremely saline area demand caution. The Ph response cannot be related to magnetic susceptibility as readily as in salt-free environments and its interpretation is complex. A reduction of DOE in high conductive environments was confirmed and this becomes increasingly important with increasing intercoil spacing. Bias of LIN approximated ECa data was evidenced though a simple correction is possible. The scope of a survey may not necessitate correcting for LIN breakdown if the LIN approximation is used, yet correction is required when comparing with true conductivity or between data from different coil configurations. Furthermore, a high signal-to-noise ratio of the Qu data caused by the extreme salinity, which amplifies the Qu response, was recognized. These results indicate that EMI surveys remain a viable option for subsurface prospection in highly saline conditions.

What is problematic regarding the assessment of shallow subsurface variability in the intertidal zone is variation in salinity and/or groundwater level. Validation should aim at providing data that allow distinction of the influences of variation in salinity and variation in texture. If

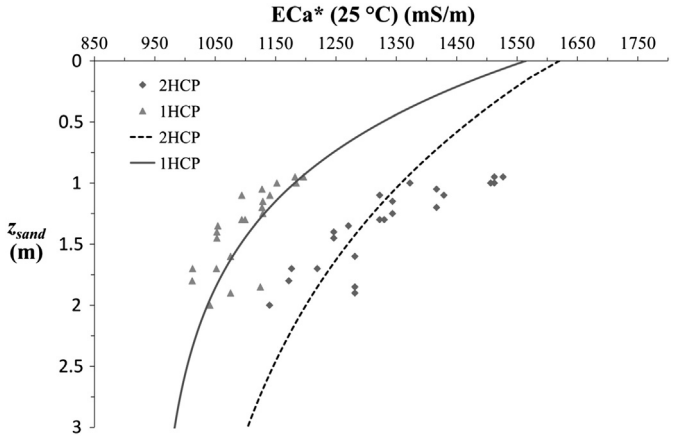

Fig. 11. Fitted cumulative depth response curves with sensor height considered (expressed as z_{sand} — ECa* (25 °C)) for the HCP coil configurations of the DUALEM-21S, with their corresponding z_{sand} observations.

there is a large variation, similar in scale, in both, interpretation will be complicated and correlation to subsurface layers compromised. Further studies of the complex relation between Ph and ECa may offer insight on this.

Though a simple correction may be applied for the LIN approximation breakdown, the LIN approximation itself can be questioned. It introduces bias in high conductive areas and contributes to the limited dynamic range for EMI measurements. Furthermore, the boundaries wherein the approximation is valid are unclear. It should be researched whether an approximation that is less susceptible to high conductivity breakdown might be developed. It is also noted that interpretation of the Qu data may be achieved without using the LIN approximation should it not be justifiable.

Acknowledgements

We would like to thank Valentijn Van Parys for aiding with the fieldwork, Rick Taylor for sharing his vast knowledge and Birger Stichelbaut for his help with orthorectification of the aerial photograph.

References

Baeteman, C., 1991. Chronology of coastal plain development during the Holocene in West Belgium. Quaternaire 2, 116–125.

Beamish, D., 2011. Low induction number, ground conductivity meters: a correction procedure in the absence of magnetic effects. J. Appl. Geophys. 75, 244–253.

Buyvenich, I.V., Jol, H.M., Fitzgerald, D.M., 2009. Coastal environments. In: Jol, H.M. (Ed.), Ground Penetrating Radar: Theory and Applications. Elsevier Science, Amsterdam, pp. 299–322.

Callegary, J.B., Ferré, T.P.A., Groom, R.W., 2007. Vertical spatial sensitivity and exploration depth of low-induction-number electromagnetic induction instruments. Vadose Zone J. 6, 158–167.

Callegary, J.B., Ferré, T.P.A., Groom, R.W., 2012. Three-dimensional sensitivity distribution and sample volume of low-induction-number electromagnetic-induction instruments. Soil Sci. Soc. Am. J. 76, 85–91.

de Jong, E., Ballantyne, A.K., Cameron, D.R., Read, D.W.L., 1979. Measurement of apparent electrical conductivity of soils by an electromagnetic induction probe to aid salinity surveys. Soil Sci. Soc. Am. J. 43, 810–812.

De Smedt, P., Van Meirvenne, M., Meerschman, E., Saey, T., Bats, M., Court-Picon, M., De Reu, J., Zwertvaegher, A., Antrop, M., Bourgeois, J., De Maeyer, P., Finke, P.A., Verniers, J., Crombé, P., 2011. Reconstructing palaeochannel morphology with a mobile multicoil electromagnetic induction sensor. Geomorphology 130, 136–141. http://dx.doi.org/10.1016/j.geomorph.2011.03.009.

Frischknecht, F.C., 1967. Fields about an oscillating magnetic dipole over a two-layer earth and application to ground and airborne electromagnetic surveys. Colo. Sch. Mines Q. 62, 1–326.

Frischknecht, F.C., Labson, V.F., Spies, B.R., Anderson, W.L., 1991. Profiling methods using small sources. In: Nabighian, M.N. (Ed.), Electromagnetic Methods in Applied Geophysics, vol. 2-A. Society of Exploration Geophysicists, USA, pp. 105–283.

Goovaerts, P., 1997. Geostatistics for natural resources evaluation. Applied Geostatistics SeriesOxford University Press, New York.

Hendrickx, J.M.H., Baerends, B., Raza, Z.I., Sadig, M., Akram Chaudhry, M., 1992. Soil salinity assessment by electromagnetic induction of irrigated land. Soil Sci. Soc. Am. J. 56, 1933–1941.

Lunne, T., Robertson, P.K., Powell, J.J.M., 1997. Cone Penetration Testing in Geotechnical Practice. Blackie Academic & Professional, London.

McNeill, J.D., 1980. Electrical conductivity of soils and rocks. Technical Note 5.Geonics Limited, Ontario.

Morris, E.R., 2009. Height-above-ground effects on penetration depth and response of electromagnetic induction soil conductivity meters. Comput. Electron. Agric. 68, 150–156.

Rhoades, J.D., Van Schilfgaarde, J., 1976. An electrical conductivity probe for determining soil salinity. Soil Sci. Soc. Am. J. 40, 647–651.

Robertson, P.K., Campanella, R.G., 1983. Interpretation of cone penetration test: part I (sand). Can. Geotech. J. 20, 1–44.

Robertson, P.K., Campanella, R.G., Gillespie, D., Greig, J., 1986. Use of piezometer cone data. Proceedings of the ASCE Specialty Conference In Situ '86: Use of In Situ Tests in Geotechnical Engineering. American Society of Engineers, Blacksburg, pp. 1263–1280.

Saey, T., Simpson, D., Vermeersch, H., Cockx, L., Van Meirvenne, M., 2009. Comparing the EM38DD and DUALEM-21S sensors for depth-to-clay mapping. Soil Sci. Soc. Am. J. 73, 7–12.

Saey, T., Van Meirvenne, M., De Smedt, P., Cockx, L., Meerschman, E., Islam, M.M., Meeuws, F., 2011. Mapping depth-to-clay using fitted multiple depth response curves of a proximal EMI sensor. Geoderma 162, 151–158.

Simpson, D., Van Meirvenne, M., Saey, T., Vermeersch, H., Bourgeois, J., Lehouck, A., Cockx, L., Vitharana, U.W.A., 2009a. Evaluating the multiple coil configurations of the EM38DD and DUALEM-21S sensors to detect archaeological anomalies. Archaeol. Prospect. 16, 91–102.

Simpson, D., Lehouck, A., Verdonck, L., Vermeersch, H., Van Meirvenne, M., Bourgeois, J., Thoen, E., Docter, R., 2009b. Comparison between electromagnetic induction and fluxgate gradiometer measurements on the buried remains of a 17th century castle. J. Appl. Geophys. 68, 294–300. http://dx.doi.org/10.1016/j.jappgeo.2009.03.006.

Slavich, P.G., Petterson, G.H., 1990. Estimating average rootzone salinity for electromagnetic (EM-38) measurements. Aust. J. Soil Res. 28, 453–463.

Spies, B.R., 1989. Effective depth of exploration in electromagnetic sounding methods. Geophysics 54, 872–888.

Tabbagh, A., 1986. Applications and advantages of the Slingram electromagnetic method for archaeological prospecting. Geophysics 51, 576–584.

van den Broeke, P.W., 1996. Turfwinning en zoutwinning langs de Noordzeekust. Een verbond sinds de ijzertijd? Tijdschr. Waterstaatsgeschied. 5, 48–59.

Wait, J.R., 1982. Geo-electromagnetism. Academic Press, New York, USA.

Williams, B.G., Baker, G.C., 1982. An electromagnetic induction technique for reconnaissance surveys of soil salinity hazards. Aust. J. Soil Res. 20, 107–118.